

Effect of hydraulic distribution on the stability of a plane slide rock slope under the nonlinear Barton-Bandis failure criterion

Lian-Heng Zhao¹, Jingyuan Cao¹, Yingbin Zhang^{*2,3} and Qiang Luo⁴

¹School of Civil Engineering, Central South University, Changsha 410075, China

²Key Laboratory of Transportation Tunnel Engineering, Ministry of Education, Southwest Jiaotong University, Chengdu, 610031, China

³Department of Geotechnical Engineering, School of Civil Engineering, Southwest Jiaotong University, Chengdu 611756, China

⁴Department of Communications of Guizhou Province, Guizhou Guiyang 550003, China

(Received July 26, 2014, Revised November 26, 2014, Accepted December 13, 2014)

Abstract. In this paper, stabilities of a plane slide rock slope under different hydraulic distributions were studied based on the nonlinear Barton-Bandis (B-B) failure criterion. The influence of various parameters on the stability of rock slopes was analyzed. Parametric analysis indicated that studying the factor of safety (*FS*) of planar slide rock slopes using the B-B failure criterion is both simple and effective and that the effects of the basic friction angle of the joint (φ_b), the joint roughness coefficient (*JRC*), and the joint compressive strength (*JCS*) on the *FS* of a planar slide rock slope are significant. Qualitatively, the influence of the *JCS* on the *FS* of a slope is small, whereas the influences of the φ_b and the *JRC* are significant. The *FS* of the rock slope decreases as the water in a tension crack becomes deeper. This trend is more significant when the flow outlet is blocked, a situation that is particularly prevalent in regions with permafrost or seasonal frozen soil. Finally, the work is extended to study the reliability of the slope against plane failure according to the uncertainty from physical and mechanics parameters.

Keywords: rock slope stability analysis; plane failure; nonlinear Barton-Bandis failure criterion; hydraulic action; factor of safety

1. Introduction

Hoek and Bray (1981) proposed the basic analytical solution for rock slope plane failures based on limit equilibrium theory. This basic solution was updated by a number of researchers considering various internal influencing factors, such as the height of the rock slope, the angle of the slope face, the angle of the failure surface, the depth of the tension crack, the shear strength of the failure surface, and the unit weight of the rock, as well as external influencing factors, such as the seismic load, surcharges, water pressure, and reinforcement effects (Ling and Cheng 1997, Kliche 1999, Rocscience 2003, Wyllie and Mah 2004, Shu *et al.* 2004, Hoek 2007, Shukla *et al.* 2009, Shukla and Hossain 2011a, b, Zhao *et al.* 2011).

However, few studies focus on the Factor of Safety (*FS*) for rock slopes with an inclined upper

*Corresponding author, Dr. Associate Professor, E-mail: yingbinz516@126.com

slope surface and inclined crack, which appear widely in engineering practice. Sharma *et al.* (1995) addressed this shortage, but Rocscience (2003) found that the equation provided in Sharma *et al.* (1995) for calculating the wedge weights is incorrect and that the factor of safety provided by the paper is not dependable.

Among the external influencing factors of slope stability, the effect of groundwater is one of the most important factors causing slope failure; therefore, the hydraulic distribution form and flow activities of underground water and its influence on the stability of rock slopes have become one of the most important topics of engineering research on rock slopes (Hoek and Bray 1981, Sharma *et al.* 1995, Wyllie and Mah 2004, Luo *et al.* 2010, Zhao *et al.* 2011). Examples illustrate that the safety factor of a saturated slope is less than 70% of the safety factor of a dry slope (Hoek and Bray 1981, Chen *et al.* 2005).

Hoek and Bray (1981) believed that the hydraulic distribution is unknown in actual rock slope engineering. Tang and Chen (2008) performed 72 sets of experiments on water pressure in a fissure to study the relationship between a static water pressure calculation formula and the aperture of the fissure. The results indicated that a complex and particular water pressure distribution formed in the tension fissure. Hoek and Bray (1981) suggested that the maximum water pressure is located at the bottom of the tension crack, and many follow-up studies (Ling and Cheng 1997, Kliche 1999, Rocscience 2003, Shu *et al.* 2004, Wyllie and Mah 2004, Hoek 2007, Shukla *et al.* 2009, Shukla and Hossain 2011a, b, Wu *et al.* 2011) corroborated this suggestion. However, this finding is not completely in conformity with practical engineering in certain situations, such as when the flow slit of a failure plane is blocked and the groundwater cannot discharge fluently through the flow slit (Luo *et al.* 2010, Zhao *et al.* 2011).

In fact, Hoek and Bray (1981) noted that there may be a more dangerous water pressure distribution in a rock slope if the slope face is iced in winter and the assumed condition of zero water pressure in the rock slope no longer exists. In this case, the water pressure at the bottom of the rock slope face should be equal to the total head of the water pressure in the rock slope. Therefore, this possibility should be established in the preliminary design stage in region where freezing conditions are possible. A similar situation occurred in southern China in the spring of 2008, when extreme snow and ice conditions appeared in a large area of Hunan, Guizhou, Sichuan, Yunan, Jiangxi, and Hubei Provinces (Wei *et al.* 2008, Yin 2008, Ma *et al.* 2008, Zhang *et al.* 2010, 2011).

Among the internal influencing factors of slope stability, the shear characteristics of the discontinuity in the rock mass are important because the discontinuity controls the deformation and destruction of the entire rock slope. Numerous project failures around the world have been caused by discontinuities in rock masses; thus, studying the shear strength of discontinuities in rock masses and their influence on rock-soil structures has important theoretical significance and engineering value. Many scholars have found that shear behavior on the rock mass structure surface cannot always satisfy the linear Mohr-Coulomb (M-C) failure criterion, which exhibits linear behavior. In particular, the shear strength given by the linear M-C criterion is significantly large when the normal stress σ_n is smaller. Because most of the vertical stresses of the rock slopes involved are small, analyzing rock slope stability with the linear M-C failure criterion may cause significant overestimation errors. Moreover, Choi and Chung (2004) noted that the joint cohesion, joint friction angle, and joint tensile strength, which are the essential input parameters in the M-C failure criterion, are not easy to obtain from laboratory tests. Therefore, it is necessary to adopt another strength criterion reflecting the nonlinear shear behavior of the discontinuity in the rock mass (Chen *et al.* 2005).

One effective model is the joint roughness coefficient – joint compression strength (*JRC-JCS*) model proposed by Barton, which estimates the shear strength parameters of structural surfaces in engineering practice (Barton 1971, Barton and Bandis 1990). However, the majority of calculation methods and numerical software applied in geotechnical engineering are established on the linear M-C failure criterion, so many studies focus on turning nonlinear Barton-Bandis (B-B) failure criterion parameters into the linear M-C failure criterion strength parameters c and φ by using the equivalent tangent method and the equivalent linear fitting method (Zhao 1998, Choi and Chung 2004, Liu *et al.* 2005, Li *et al.* 2009).

Only a few researchers have studied the stability of rock slopes based on the B-B failure criterion. Miller (1988) and Rocscience (2003) analyzed the stability of rock slopes without tension cracks against planar failure based on the B-B failure criterion under simple conditions. However, the analysis results of the safety factor were incorrect when at an $(\tau/\sigma_n) > 70^\circ$ (here τ is the peak strength and σ_n is the effective normal stress on the failure plane) (Rocscience 2003, Chen *et al.* 2005, Nagpal and Basha 2012).

There are many uncertainties in stability analysis of rock slope, which has influence on the analysis results. One the shortcoming of the conventional *FS* used in the rock slope stability analysis is that it does not reflect the uncertainty of the rock mass parameters. Some researchers have contributed to the subject of reliability of rock slopes with B-B failure criterion (Feng and Lajtai 1997, Nagpal and Basha 2012, Sharma and Basha 2012, Basha and Moghal 2013). Feng and Lajtai (1997) analyze the effect of parameter variability with EzSlide through the use of the Monte Carlo simulation technique. Nagpal and Basha (2012) developed a reliability approach, in which the resisting forces of the sliding plane are calculated using Barton's theory to analyze the stability of anchored rock slopes against planar failure. Sharma and Basha (2012) and Basha and Moghal (2013) summarized the development of a methodology and reliability-based LRFD guidelines (the Load Resistance Factor Design) for rock slopes against wedge failures, and Barton's model was used to derive analytical expressions for the *FS*.

This paper aims to derive the effect of different water pressure distribution forms and nonlinear B-B failure criteria on the stability of translational sliding in rock slopes with an inclined upper slope surface and crack. The influence of various parameters on the stability of rock slopes was analyzed. Similar as Feng and Lajtai (1997), Nagpal and Basha (2012), Sharma and Basha (2012) and Basha and Moghal (2013), the work is also extended to study the reliability of the rock slope against plane failure according to the uncertainty of calculation parameters (e.g., material strength, joint geometry and pore water pressures).

2. Nonlinear Barton-Bandis failure criterion of the structural plane

There are two methods to estimate the shear strength of the discontinuity in rock masses (Ladanyi and Archambault 1970, Barton 1971, Jaeger 1971, Barton and Bandis 1990, Chen *et al.* 2005). The first method describes the mechanical mechanism of the shear strength formula for the structural surface by analyzing the empirical formula, which is summarized from direct shear tests of the structural surface. The second method proposes a theoretical formula of shear strength for the structural surface based on a theoretical analysis of the structural shear strength, and a test is conducted to verify the effectiveness of this method. The former formula for the shear strength of the structure surface is an estimating test, such as the Patton formula, Jaeger formula, and Barton formula; the latter is an estimating theory, such as the Ladanyi formula (Chen *et al.* 2005).

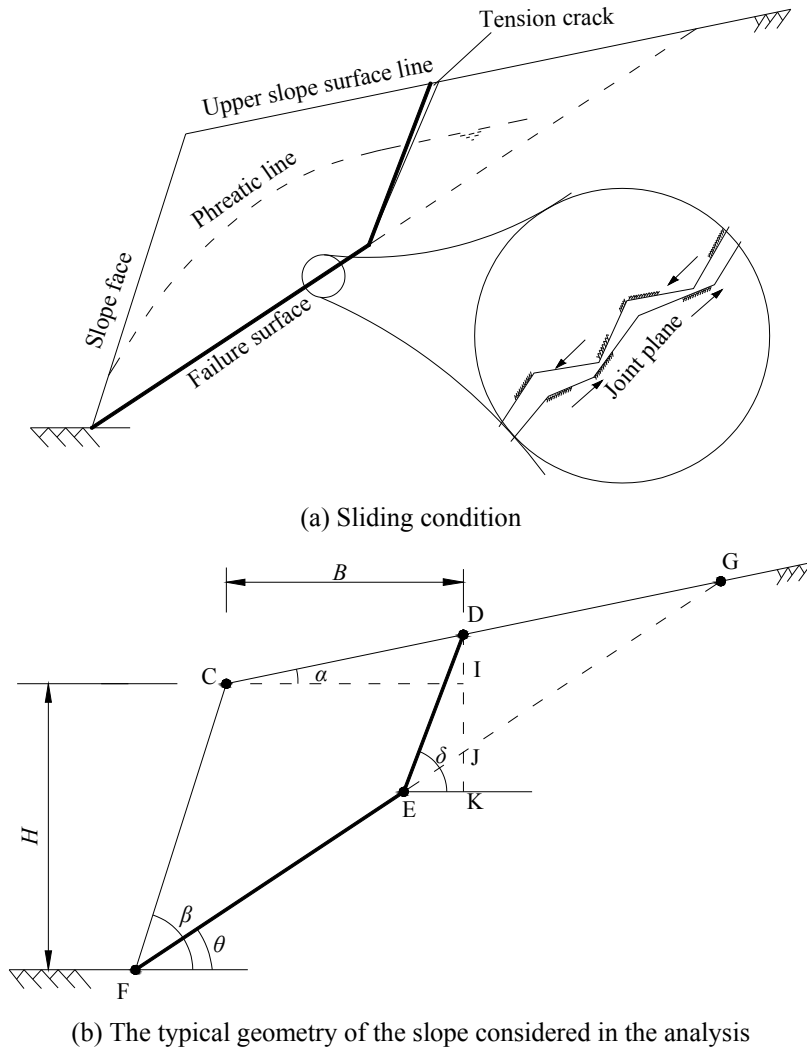


Fig. 2 Typical geometry for the translational sliding failure mechanism in a hard rock slope in present study

in a rock slope, as shown in Fig. 1, in which the upper slope surface is horizontal and the tension crack is vertical. The translational sliding failure mode proposed by Hoek and Bray (1981) was improved in Sharma *et al.* (1995) and Rocscience (2003), as shown in Fig. 2, in which the upper slope surface and crack are inclined. Slope stability is studied as a two-dimensional problem considering a slice of the unit thickness through the slope with the basic computational formula and hypotheses, as suggested by Hoek and Bray (1981), Sharma *et al.* (1995) and Rocscience (2003).

The slope geometry is defined in Fig. 2. The various symbols used in this figure are as follows: β , the slope dip; θ , the failure plane dip; H , the slope height; B , the distance from the crack to the crest of the slope; α , the upper slope surface dip; and δ , the crack dip. The details of the derivation of slope geometry (trigonometric calculations) are presented in the Appendix.

3.2 Hydraulic distribution form and water pressure calculation

Using Hoek and Bray's (1981) suggestions, the water force in crack V and the water force in a failure plane U can be calculated using the water pressure in the tension crack and failure plane. Because the hydraulic distribution form is much more complex than the water pressure distribution hypothesis, it is crucial to make reasonable assumptions regarding the hydraulic distribution form based on the actual situation of the slope.

The water force is calculated according to the following three working conditions in this paper: **Case 1**: maximum water pressure at the base of the crack, as shown in Fig. 3; **Case 2**: maximum water pressure at the toe, as shown in Fig. 4; **Case 3**: maximum water pressure at mid height, as shown in Fig. 5.

The physical interpretations for the three hydraulic distribution forms are as follows (Rocscience 2003, Shu *et al.* 2004, Zhao *et al.* 2011, Wu *et al.* 2011). For **Case 1**, suppose that the degree of opening of the failure plane is small or nonexistent. If the volume of water in the tension crack is greater than that of the discharge water, hydrostatic pressure can suddenly increase at the bottom of the tension crack, in accordance with the first water pressure distribution case. For **Case 2**, suppose that the flow slit of the failure plane is blocked or water discharge breaks down in a region with permafrost or seasonal frozen soil. Groundwater cannot discharge through the flow outlet freely at the bottom of the sliding body, and the water pressure at the bottom of the sliding surface will increase sharply, in accordance with the second water pressure distribution case. For **Case 3**, suppose that the degree of opening of the failure plane is large and the volume of water in the crack and failure plane is less than that of the discharge water. The maximum water pressure point in the crack or the failure plane will gradually change with time, in accordance to the third water pressure distribution case.

Case 1: MAXIMUM PRESSURE AT THE BASE OF THE TENSION CRACK

The symbols used in this figure are γ_w , the water unit weight, and Z_w , the depth of the water in the tension crack.

The water force on crack DE can be expressed as follows

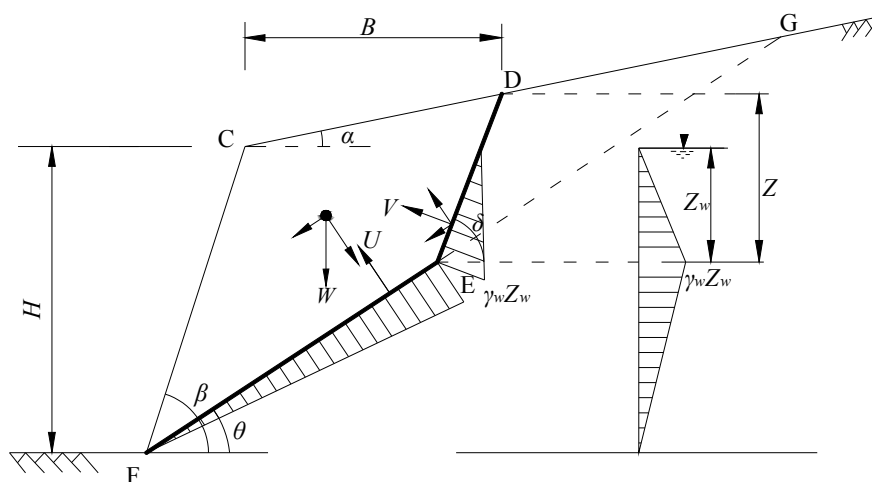


Fig. 3 **Case 1**: Maximum water pressure at base of tension crack

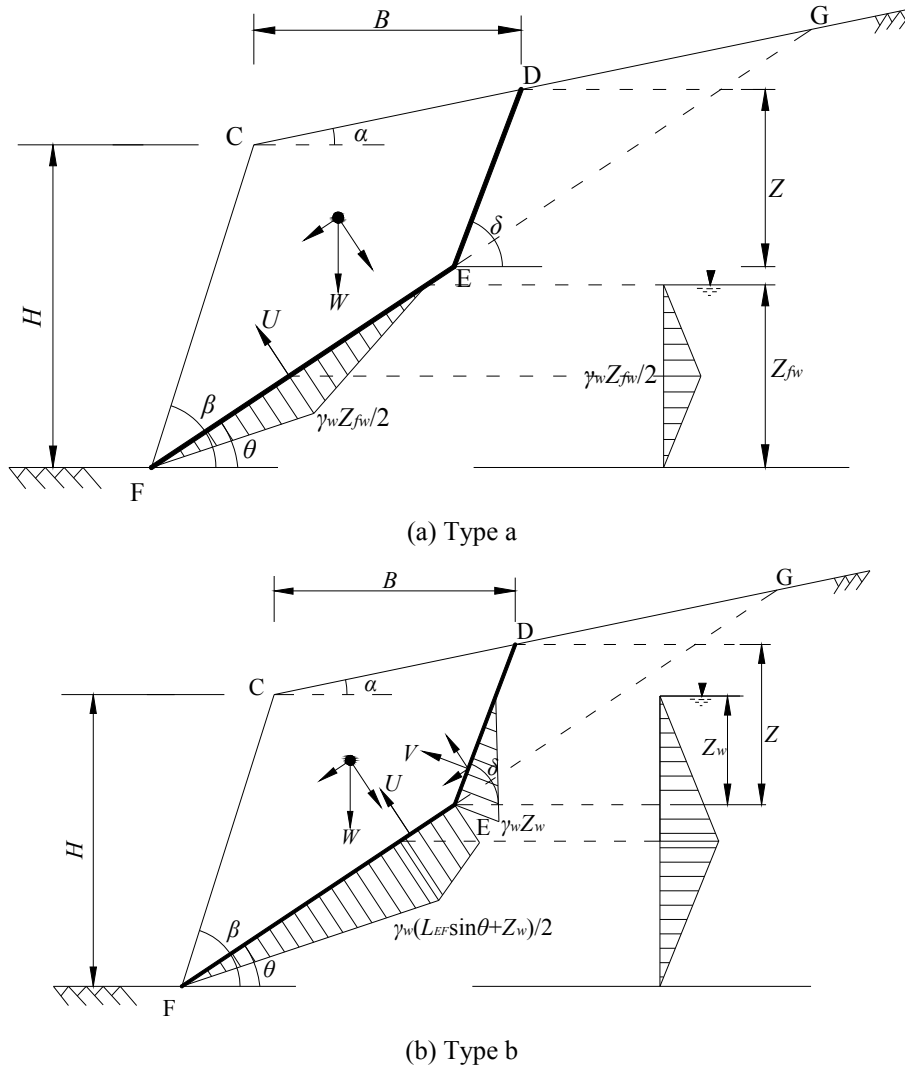


Fig. 5 Case 3: Maximum water pressure at mid height

Case 2: MAXIMUM PRESSURE AT THE TOE

The symbol used in this figure, Z_{fw} , represents the depth of the water on the failure surface.

There are two types of water pressure distributions along the crack and the base of failure surface.

Type a: $Z_w \neq 0$

The water force on crack DE can be expressed as follows

$$V_{DE} = \frac{1}{2} \gamma_w Z_w \cdot \frac{Z_w}{\sin \delta} \tag{4}$$

The water force on failure plane EF can be expressed as follows

$$U_{EF} = \frac{[\gamma_w Z_w + \gamma_w (L_{EF} \sin \theta + Z_w)] \cdot L_{EF}}{2} \quad (5)$$

Type b: $Z_w = 0$ and $Z_{fw} \leq L_{EF} \sin \theta$

The water force on crack DE can be expressed as follows

$$V_{DE} = 0 \quad (6)$$

The water force on failure plane EF can be expressed as follows

$$U_{EF} = \frac{\gamma_w \cdot Z_{fw}^2}{2 \sin \theta} \quad (7)$$

Case 3: MAXIMUM PRESSURE AT MID HEIGHT

There are three types of water pressure distributions along the crack and the base of failure surface.

Type a: $Z_w = 0$ and $Z_{fw} \leq L_{EF} \sin \theta$

The water force on crack DE can be expressed as follows

$$V_{DE} = 0 \quad (8)$$

The water force on failure plane EF can be expressed as follows

$$U_{EF} = \frac{\gamma_w \cdot Z_{fw}^2}{4 \sin \theta} \quad (9)$$

Type b: $Z_w \neq 0$ and $Z_w \leq (L_{EF} \sin \theta + Z_w)/2$

The water force on crack DE can be expressed as follows

$$V_{DE} = \frac{1}{2} \gamma_w Z_w \cdot \frac{Z_w}{\sin \delta} \quad (10)$$

The water force on failure plane EF can be expressed as follows

$$U_{EF} = \frac{\gamma_w [(L_{EF} \sin \theta + 3Z_w)(L_{EF} \sin \theta - Z_w) + (L_{EF} \sin \theta + Z_w)^2]}{8 \sin \theta} \quad (11)$$

Type c: $Z_w \neq 0$ and $Z_w \geq (L_{EF} \sin \theta + Z_w)/2$

The water force on crack DE can be expressed as follows

$$V_{DE} = \frac{\gamma_w [(3L_{EF} \sin \theta + Z_w)(Z_w - L_{EF} \sin \theta) + (L_{EF} \sin \theta + Z_w)^2]}{8 \sin \delta} \quad (12)$$

The water force on failure plane EF can be expressed as follows

$$U_{EF} = \frac{\gamma_w \cdot L_{EF}^2 \cdot \sin \theta}{2} \quad (13)$$

3.3 Factor of safety

This problem considers the force equilibrium without considering any resistance to sliding at the lateral boundaries of the sliding block. The Factor of Safety (FS) of the rock plane slope is defined as follows (Hoek and Bray 1981, Sharma *et al.* 1995, Wyllie and Mah 2004, Hoek 2007)

$$FS = \frac{F_{\text{resist}}}{F_{\text{induce}}} \quad (14)$$

where F_{resist} is the total force available to resist sliding and F_{induce} is the total force tending to induce sliding.

From Fig. 2, the normal stress acting on the failure plane EF is calculated as follows

$$\sigma_n = \frac{W_{CDEF} \cos \theta - U_{EF} - V_{DE} \cos(\delta - \theta)}{L_{EF}} \quad (15)$$

where W_{CDEF} is the weight of the sliding wedge $CDEF$ (kN) and can be found in Appendix.

When the shear strength of the sliding failure plane can be defined in terms of the M-C failure criterion, the total force available to resist sliding is calculated as follows

$$F_{\text{resist}} = \tau \cdot L_{EF} = c \cdot L_{EF} + [W_{CDEF} \cos \theta - U_{EF} - V_{DE} \cos(\delta - \theta)] \tan \varphi \quad (16)$$

where c is the cohesiveness of the failure plane (kPa) for the linear M-C failure criterion, φ is the friction angle of the failure plane ($^\circ$) for the M-C failure criterion.

The total force tending to induce sliding is calculated as follows

$$F_{\text{induce}} = W_{CDEF} \sin \theta + V_{DE} \sin(\delta - \theta). \quad (17)$$

Substituting Eqs. (16)-(17) into Eq. (14), the FS of slope can be calculated as follows

$$FS = \frac{c \cdot L_{EF} + [W_{CDEF} \cos \theta - U_{EF} - V_{DE} \cos(\delta - \theta)] \tan \varphi}{W_{CDEF} \sin \theta + V_{DE} \sin(\delta - \theta)}. \quad (18)$$

When the shear strength of the sliding failure plane can be defined in terms of the nonlinear JRC - JCS empirical formula, according to Eq. (1), the total force available to resist the sliding of rigid body $CDEF$ is calculated as follows

$$\begin{aligned} F_{\text{resist}} &= \tau \cdot L_{EF} \\ &= \left\{ \sigma_n \tan \left[\varphi_b + JRC \log_{10} \left(\frac{JCS}{\sigma_n} \right) \right] \right\} \cdot L_{EF} \\ &= [W_{CDEF} \cos \theta - U_{EF} - V_{DE} \cos(\delta - \theta)] \times \tan \left\{ \varphi_b + JRC \log_{10} \left[\frac{JCS}{\frac{W_{CDEF} \cos \theta - U_{EF} - V_{DE} \cos(\delta - \theta)}{L_{EF}}} \right] \right\} \end{aligned} \quad (19)$$

$$FS = \frac{\left[\begin{array}{l} W_{CDEF} \cos \theta - k_h W_{CDEF} \sin \theta - U_{EF} \\ - V_{DE} \cos(\delta - \theta) + T \sin(\omega + \theta) + qB \cos \theta \end{array} \right] \times \tan \left\{ \phi_b + JRC \log_{10} \left[\frac{JCS}{\frac{W_{CDEF} \cos \theta - k_h W_{CDEF} \sin \theta - U_{EF} - V_{DE} \cos(\delta - \theta) + T \sin(\omega + \theta) + qB \cos \theta}{L_{EF}}} \right] \right\}}{W_{CDEF} \sin \theta + k_h W_{CDEF} \cos \theta + V_{DE} \sin(\delta - \theta) - T \cos(\omega + \theta) + qB \sin \theta} \quad (22)$$

4. Verification calculation and analysis

In this section, example calculations and analyses are carried out to validate the present method in this section.

Example calculation 1: Consider that $H = 60$ m, $\beta = 50^\circ$, $\theta = 35^\circ$, $\alpha = 0-30^\circ$, $\delta = 70-90^\circ$, $Z_w = 14$ m, $\gamma_R = 26$ kN/m³, $\gamma_w = 10$ kN/m³, $c = 120$ kPa, $\phi = 45^\circ$, and the distance from the crack to crest B is equal to 15.33576 m. The hydraulic distribution form and water pressure calculations follow the working conditions of **Case 1**. A comparison of the results with Sharma *et al.* (1995) and Rocscience (2003) is provided in Table 1.

Table 1 FS calculated by Rocscience (2003) (R03), Sharma *et al.* (1995) (S95) and this study

Upper slope surface angle (°)	Tension crack angle (°)	Weight (t)			Percent filled (%)			Factor of safety		
		SR95	R03	This study	S95	R03	This study	S95	R03	This study
0	70	2267.68	2267.76	2267.757	-	74	65.755	1.60	1.570	1.567
10	70	3317.43	2268.91	2268.915	-	62	55.116	1.54	1.565	1.561
15	70	4433.85	2265.85	2265.850	-	58	50.842	1.51	1.553	1.558
20	70	6715.23	2259.95	2259.947	-	53	47.020	1.48	1.558	1.555
25	70	12998.24	2250.62	2250.624	-	49	43.533	1.45	1.555	1.552
30	70	71425.55	2236.97	2236.970	-	46	40.290	1.43	1.543	1.549
0	80	2340.37	2341.05	2341.055	-	87	84.955	1.58	1.583	1.579
10	80	3456.77	2373.24	2373.240	-	73	71.210	1.53	1.578	1.575
15	80	4636.49	2388.45	2388.453	-	68	65.687	1.50	1.570	1.572
20	80	7032.68	2403.29	2403.289	-	63	60.750	1.48	1.567	1.570
25	80	13465.16	2417.85	2417.853	-	58	56.244	1.45	1.568	1.568
30	80	46627.40	2432.20	2432.198	-	54	52.055	1.43	1.562	1.566
0	90	2391.03	2392.38	2392.378	-	100	99.935	1.58	1.586	1.587
10	90	3558.34	2446.29	2446.289	-	84	83.766	1.53	1.581	1.583
15	90	4785.03	2474.30	2474.301	-	77	77.270	1.50	1.584	1.582
20	90	7254.02	2503.66	2503.659	-	71	71.462	1.48	1.584	1.580
25	90	13932.64	2534.95	2534.948	-	66	66.162	1.45	1.579	1.578
30	90	47526.01	2568.90	2568.898	-	61	61.234	1.43	1.578	1.576

The results from the present study are the same as those provided in Rocscience (2003), but there are large differences with the results provided in Sharma *et al.* (1995). According to the study of Rocscience (2003), the equation provided in Sharma *et al.* (1995) for calculating the wedge weights is incorrect and the safety factor provided by Sharma *et al.* (1995) is not reliable.

Example calculation 2: Consider a dry plane slide rock slope without crack (see Fig. 7) where $\beta = 64^\circ$, $\theta = 35-50^\circ$, $\gamma_R = 27 \text{ kN/m}^3$, $H = 3, 6, 15, \text{ and } 30 \text{ m}$, $\phi_b = 32^\circ$, $JCS = 100 \text{ Mpa}$, and $JRC = 3, 7, \text{ and } 11$. The computed values by Rocscience (2003), Miller (1988) and the present study are listed in Table 2.

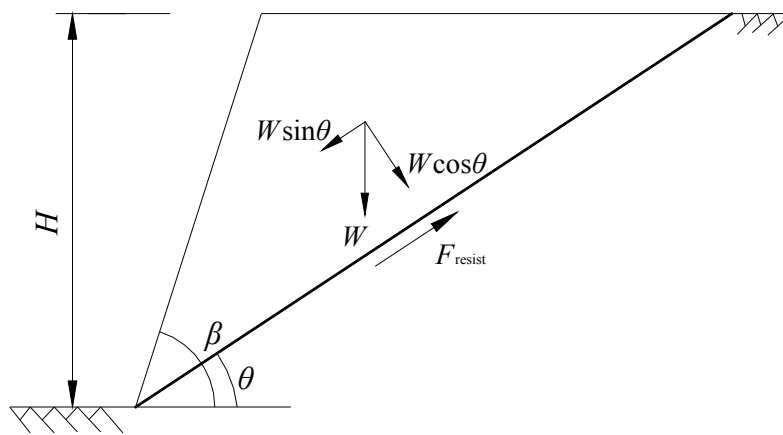


Fig. 7 A dry translational sliding in a hard rock slope without tension crack

Table 2 The FS values calculated by Rocscience (2003), Miller (1988) and present study

JRC	H (m)	Factor of safety					
		$\theta = 35^\circ$			$\theta = 50^\circ$		
		Miller (1988)	Rocscience (2003)	This study	Miller (1988)	Rocscience (2003)	This study
3	30	1.21	1.209	1.209	0.74	0.741	0.741
	15	1.25	1.248	1.248	0.76	0.765	0.765
	6	1.30	1.301	1.301	0.80	0.798	0.798
	3	1.34	1.343	1.343	0.82	0.824	0.824
7	30	1.78	1.778	1.778	1.16	1.158	1.158
	15	1.92	1.919	1.919	1.26	1.253	1.253
	6	2.13	2.127	2.127	1.40	1.395	1.395
	3	2.31	2.306	2.306	1.52	1.519	1.519
11	30	2.72	2.711	2.711	1.96	1.948	1.948
	15	3.15	3.138	3.138	2.32	2.307	2.305
	6	3.92	3.904	3.904	3.02	3.003	2.305
	3	4.76	4.736	3.924	3.87	3.848	2.305

According to Hoek and Bray (1981), the most suitable stress level range of the nonlinear B-B failure criterion is $0.01 < \sigma_n / \sigma_c < 0.3$ and the maximum of the brackets in Eq. (1) should be less than 70° . That is, when $\text{atan}(\tau / \sigma_n) > 70^\circ$ (i.e., $[\varphi_b + JRC \log_{10}(JCS / \sigma_n)] > 70^\circ$), $[\varphi_b + JRC \log_{10}(JCS / \sigma_n)]$ is assumed to be 70° . Therefore, some of safety factor values calculated by Rocscience (2003) and Miller (1988) should be revised as shown in Table 2.

5. Calculation and parameter analysis

5.1 Influence of the Barton-Bandis failure criterion parameters on the stability analysis

In this section, parametric study is carried out to investigate the effect of B-B failure criterion parameters on the stability analysis of rock slopes.

Consider a dry plane slide rock slope with vertical tension crack and horizontal upper slope

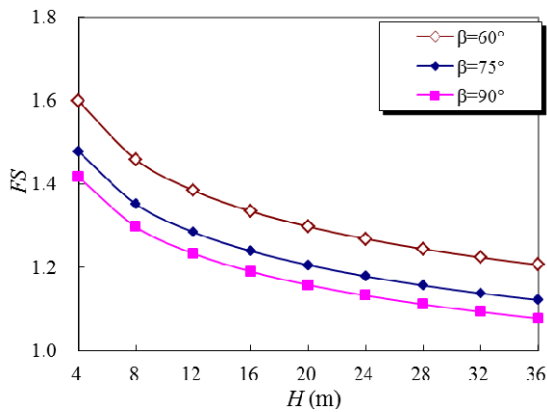


Fig. 8 The FS as a function of the slope height

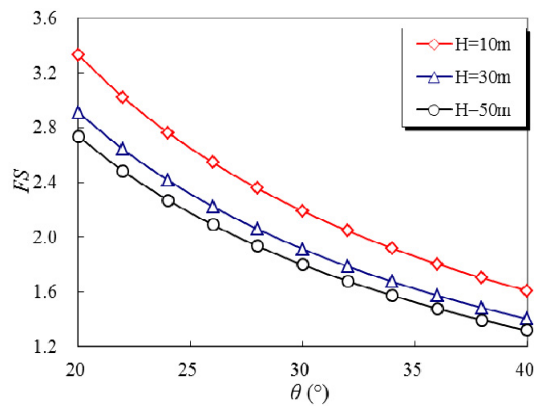


Fig. 9 The FS as a function of the sliding plane dip angle

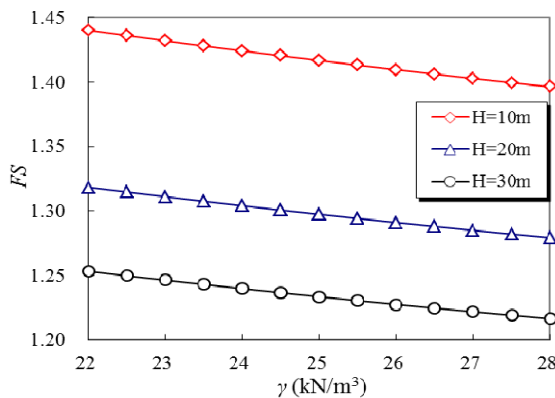


Fig. 10 The FS as a function of the rock bulk density

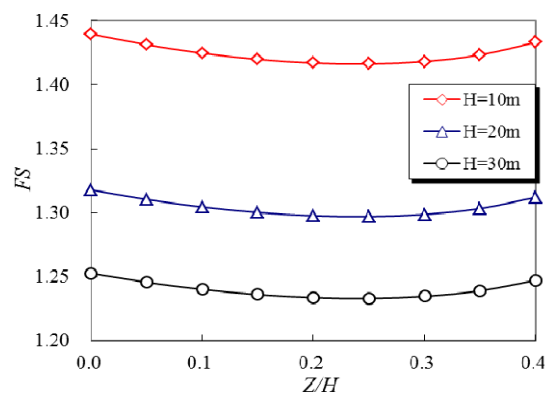
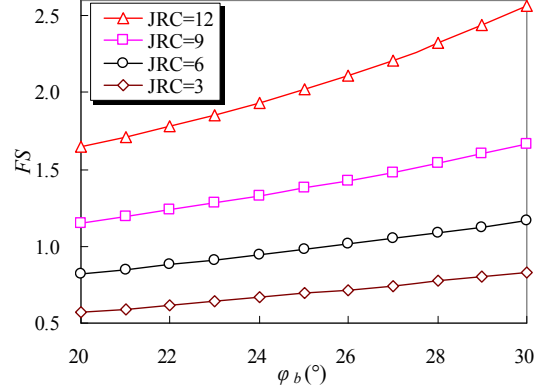
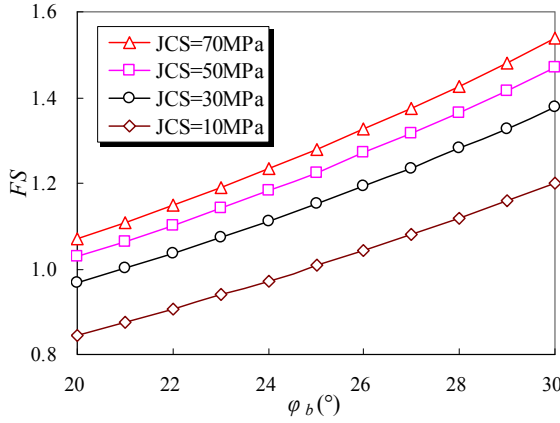


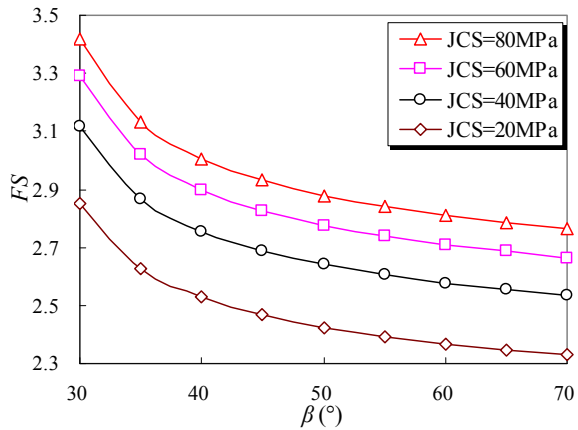
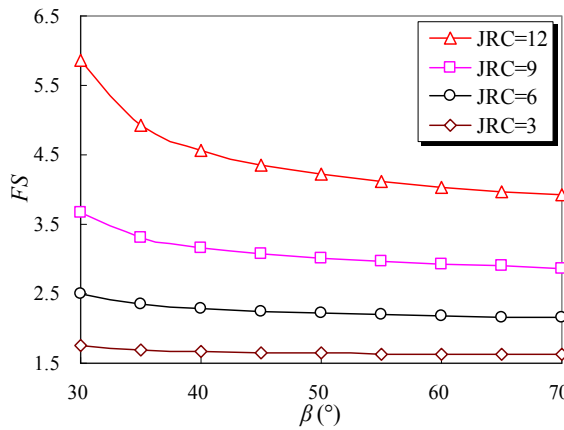
Fig. 11 The FS as a function of the tension crack length ratio to the slope height angle



(a) The effect of ϕ_b and JCS on the factor of safety

(b) The effect of ϕ_b and JRC on the factor of safety

Fig. 12 The FS as a function of the basic friction angle of joint



(a) The effect of the β and the JRC on the factor of safety

(b) The effect of β and the JCS on the factor of safety

Fig. 13 The FS as a function of the slope dip angle

Table 3 Calculation parameters

Serial number of figure	ϕ_b (°)	JCS (MPa)	JRC	H (m)	β (°)	θ (°)	γ_R (kN/m ³)	Z/H (m)	α (°)	δ (°)
Fig. 8	29	50	8	4~36	60~90	45	25	0.2	0	90
Fig. 9	29	50	8	10~50	60	20~40	25	0.2	0	90
Fig. 10	29	50	8	10~30	60	45	22~28	0.2	0	90
Fig. 11	29	30	8	10~30	60	45	25	0.0~0.4	0	90
Fig. 12(a)	20~30	10~70	8	10	60	45	25	0.2	0	90
Fig. 12(b)	20~30	50	3~12	10	60	45	25	0.2	0	90
Fig. 13(a)	29	50	3~12	10	30~70	25	25	0.2	0	90
Fig. 13(b)	29	20~80	8	10	30~70	25	25	0.2	0	90

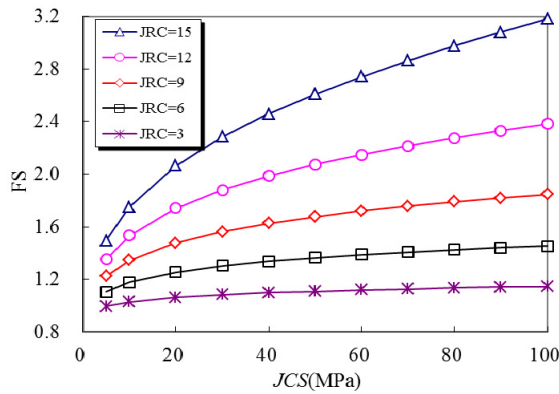


Fig. 14 The *FS* as a function of the joint roughness coefficient (*JRC*) and the joint compressive strength (*JCS*)

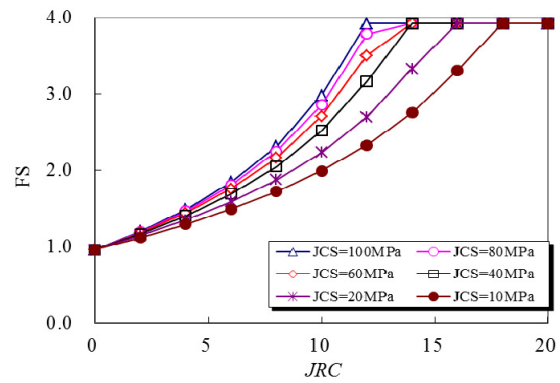


Fig. 15 The *FS* as a function of the joint roughness coefficient (*JRC*) and the joint compressive strength (*JCS*). Note: According to Hoek and Bray (1981), When $[\varphi_b + JRC \log_{10} (JCS / \sigma_n)]$ is greater than 70° , make it equal to 70°

Table 4 Calculation parameters

Serial number of figure	φ_b (°)	<i>JCS</i> (MPa)	<i>JRC</i>	<i>H</i> (m)	β (°)	θ (°)	γ_R (kN/m ³)	<i>B</i> (m)	α (°)	δ (°)
Fig. 14	32	5~100	3~15	60	64	35	27	20	15	70
Fig. 15	34	10~100	0~20	30	45	35	27	15	15	70

surface, Figs. 8-13 presents the changes in the *FS* for varied case parameters as shown in Table 3. Consider a dry plane slide rock slope with inclined crack and inclined upper slope surface, Figs. 14-15 presents the changes in the *FS* for varied case parameters as shown in Table 4.

Figs. 8-15 illustrate that the *FS* of the slope decreases with increasing slope height and unit weight of the rock mass. The effect of the unit weight is not discernible. Moreover, when φ_b , *JRC*, and *JCS* increase, the *FS* exhibits a significant upward trend; however, when the other conditions are the same, the *FS* decreases first and then increases with increases in the inclination angle of the slope and the depth of the tension crack at the top of the slope. It is found that *JCS* in Eq. (32) is \log_{10} (of *JCS*), so the effect of this parameter on the *FS* is smaller. The outstanding impact on the *FS* is due to φ_b and *JRC*.

5.2 Influence of the hydraulic form on the stability of slope

The influence of the hydraulic form on the stability of the slope is investigated in this section by considering the influence of the occurrence of different hydraulic forms.

Changes in the *FS* for the planar failure rock slope when $H = 60$ m, $\beta = 64^\circ$, $\theta = 35^\circ$, $\gamma_R = 27$ kN/m³, $\gamma_w = 10$ kN/m³, $B = 20$ m, $\alpha = 15^\circ$, $\delta = 70^\circ$, $\varphi_b = 32^\circ$, *JCS* = 100 MPa, *JRC* = 9, the rock slope has three different hydraulic distribution forms, $Z_w + Z_{wf} = 0-65.3590$ m, and $Z_w = 0-41.4201$ m ($L_{DE} \times \sin\delta = 41.4201$ m) (when $Z_w = 0$, $Z_{wf} = 23.9389$ m ($L_{EF} \times \sin\theta = 23.9389$ m) in **Cases 2** and **Cases 3**) are shown in Fig. 16.

Fig. 16 illustrates that the hydraulic distribution form, the water depth in the tension crack, and

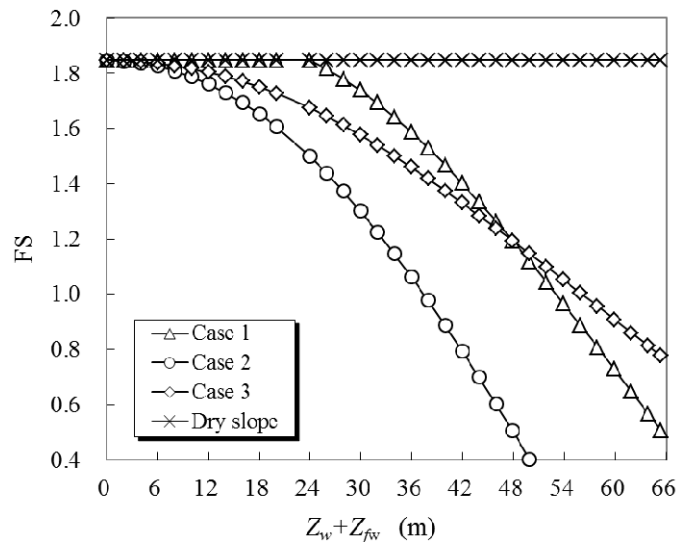


Fig. 16 The FS versus depth of water in tension crack for different water pressure distribution conditions

the failure plane have a significant influence on the stability of the rock slope. A rock slope will have a smaller FS as the water in the crack becomes deeper. Furthermore, the influence of this phenomenon is more significant when the flow outlet is blocked (**Case 2**). When the flow outlet is blocked, groundwater cannot discharge through the flow outlet at the bottom of the sliding body, and the water pressure in the sliding surface increases sharply. The FS of the rock slope might exceed the expected results, particularly in regions with permafrost or seasonal frozen soil. In the case that the sliding surface flow outlet is not blocked, the FS for the traditional hydraulic distribution form (**Case 1**) is slightly larger than that for the modified hydraulic distribution form (**Case 3**) when the water in the tension crack is shallower. The outcome is the opposite when the water in the crack is deeper.

6. Reliability analysis

The traditional deterministic analysis method cannot exactly reflect the uncertainty and complexity of geotechnical properties by only taking the mean parameter values of rock masses for calculation. A more rational approach is to compute a reliability index β , similar methodology as reported by Nagpal and Basha (2012), Sharma and Basha (2012) and Basha and Moghal (2013) is adopted for the reliability-based analysis of rock slopes against plane failure in the present paper. The minimum reliability index β is determined by the Monte Carlo simulation technique in this paper (Fenton and Griffiths 2008).

Consider a dry plane slide rock slope with $H = 60$ m, $\beta = 64^\circ$, $\theta = 35^\circ$, $\alpha = 15^\circ$, $B = 20$ m, $\gamma_R = 27$ kN/m³ are regarded as constant parameters, only a limited number of random variables considered are shown in Table 5 refer to the study of Feng and Lajtai (1997), Nagpal and Basha (2012), Sharma and Basha (2012) and Basha and Moghal (2013). The effect on minimum reliability index (β) due to the change in coefficient of variation of the nonlinear B-B failure criterion parameters JRC , JCS , φ_b and the crack dip δ is shown in Fig. 17.

Table 5 Calculation parameters for Fig. 17

Serial number of figure	Random variables	Mean	Coefficient of variation (COV) (in %)	Distribution
Fig. 17 (a)	<i>JRC</i>	4~16	5~30	Log-normal
	<i>JCS</i>	10 (MPa)	30	Log-normal
	φ_b	32 (°)	15	Log-normal
	δ	70 (°)	5	Normal
Fig. 17 (b)	<i>JRC</i>	9	10	Log-normal
	<i>JCS</i>	10~100 (MPa)	5~30	Log-normal
	φ_b	32 (°)	15	Log-normal
	δ	70 (°)	5	Normal
Fig. 17 (c)	<i>JRC</i>	9	10	Log-normal
	<i>JCS</i>	10 (MPa)	30	Log-normal
	φ_b	20~40 (°)	2~30	Log-normal
	δ	70 (°)	5	Normal
Fig. 17 (d)	<i>JRC</i>	9	10	Log-normal
	<i>JCS</i>	10 (MPa)	30	Log-normal
	φ_b	32 (°)	15	Log-normal
	δ	60~78 (°)	5~30	Normal

Fig. 17 illustrate that the reliability index (β) decreases greatly with the increasing variability for *JRC* and φ_b , the increasing variability for *JCS* does not much affect the reliability index (β) and the increasing variability for δ have minor influence on reliability index (β).

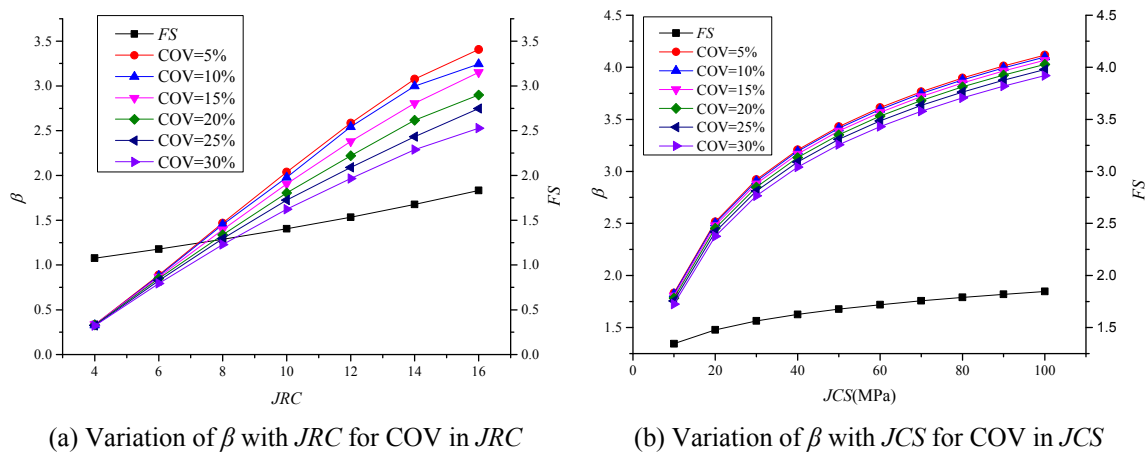


Fig. 17 Variation of reliability index (β) with different parameters (*JRC*, *JCS*, φ_b , δ) for COV in different parameters (*JRC*, *JCS*, φ_b , δ)

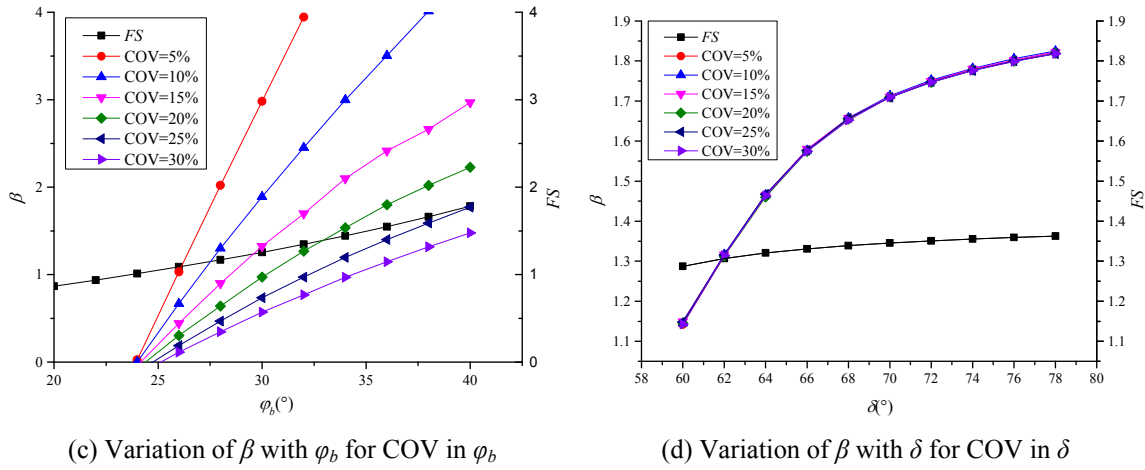


Fig. 17 Continued

Table 6 Calculation parameters for Fig. 18

Serial number of Fig. 6	Random variables	Mean	Coefficient of variation (COV) (in %)	Distribution
Fig. 18	$Z_w + Z_{fw}$	2-44 (m)	5~30	Normal
	JRC	9	10	Log-normal
	JCS	10 (MPa)	30	Log-normal
	ϕ_b	32(°)	15	Log-normal

Consider that $H=60$ m, $\beta=64^\circ$, $\theta=35^\circ$, $\alpha=15^\circ$, $\delta=70^\circ$, $B=20$ m, $\gamma_R=27$ kN/m³, $\gamma_w=10$ kN/m³ are regarded as constant parameters, and the random variables considered are shown in Table 6. For three different hydraulic forms (**Cases 1**, **Cases 2** and **Cases 3**), the effect on minimum

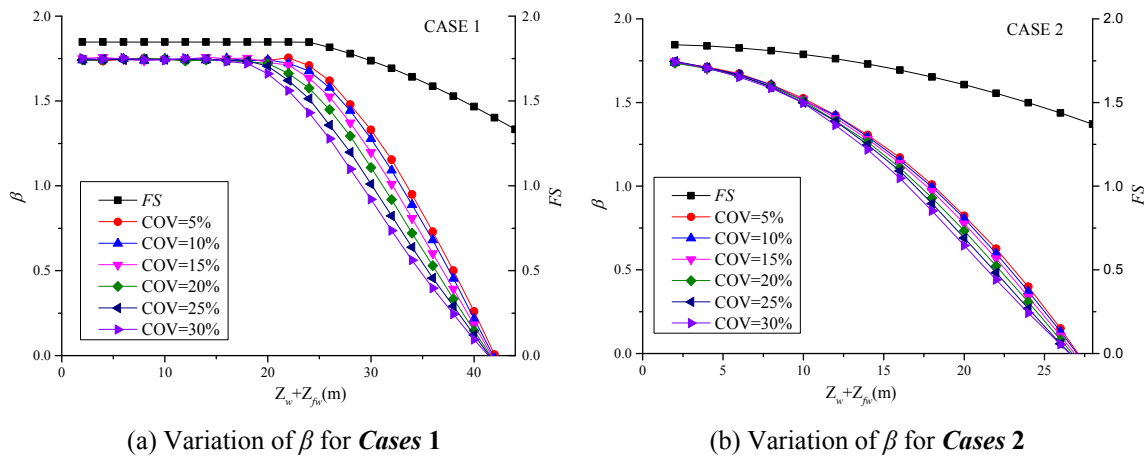


Fig. 18 Variation of β with $Z_w + Z_{wf}$ for COV in $Z_w + Z_{wf}$ for different hydraulic forms

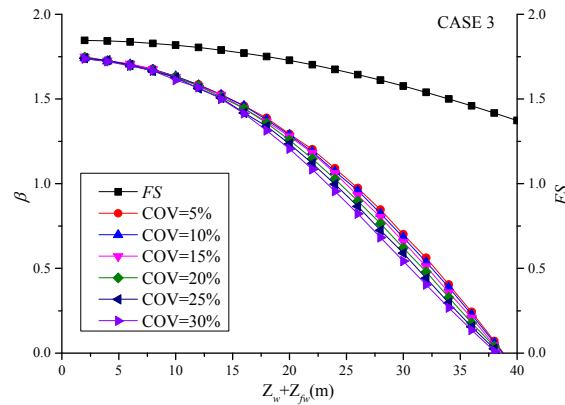
(c) Variation of β for *Cases 3*

Fig. 18 Continued

reliability index (β) due to the change in coefficient of variation of $Z_w + Z_{wf}$ is shown in Fig. 18.

Fig. 18 illustrates that although the increasing variability for $Z_w + Z_{wf}$ does not affect the reliability index (β) greatly, the groundwater will obviously lead to the decrease of the reliability index (β), especially in the least favorable hydraulic distribution form (*Cases 2*) that the flow outlet is blocked.

7. Conclusions

- (1) φ_b , JRC , and JCS have a significant impact on the stability of the rock slope. Relatively speaking, the influence of a change in JCS on the FS of slope is small, whereas the influences of φ_b and JRC on the FS of the slope are significant.
- (2) The hydraulic distribution form, the water depth in the crack, and the failure plane has a significant influence on the stability of the rock slope. A rock slope will have a smaller FS as the water in the crack becomes deeper. The influence of this phenomenon is more significant when the flow outlet is blocked (*Case 2*), a situation that is particularly prevalent in regions with permafrost or seasonal frozen soil. In the case that the sliding surface flow outlet is not blocked, using the calculation results of the FS from the traditional hydraulic distribution form (*Case 1*) would lead to an incorrect evaluation of slope stability.
- (3) According to the uncertainty of rock masses parameters, the reliability analysis of the rock slope against plane failure has been carried out. The reliability index (β) decreases greatly with the increasing variability for JRC and φ_b , the rise of groundwater level also obviously led to the decrease of the reliability index (β), especially that the flow outlet is blocked.

Over time, if the failure plane of a rock slope is filled with some type of weak material, the shear strength of the filling structure is determined by the shear strength of the filling substance itself, the wall strength of the structure surface, the thickness of the filling, structural surface undulations, and other factors. In addition, the rock slope is not always controlled by a single sliding surface; further analysis of the stability of rock slopes composed of a multi-slip structure

surface and affected by the infill in the structural surface is required.

Acknowledgments

The authors gratefully acknowledge the financial support provided by the National Natural Science Foundation of China (No. 51208522, 51408511), the National Basic Research Program of China (973 Program) (No. 2013CB036204) and the opening fund of State Key Laboratory of Geohazard Prevention and Geoenvironment Protection (Chengdu University of Technology) (No. SKLGP2014K015). The authors particularly thank Miss Gao, Y.Y. and Miss Zhang, T., who were a constant help to the authors.

References

- Barton, N.R. (1971), "A relationship between joint roughness and joint shear strength", *Proceedings of International Symposium on Rock Mechanics*, Nancy, France, October, pp. 1-8.
- Barton, N.R. and Bandis, S. (1990), "Review of predictive capabilities of JRC-JCS model in engineering practice", *Proceedings of International Conference on Rock Joints*, Leon, Norway, pp. 603-610.
- Basha, B.M. and Moghal, A.A.B. (2013), "Load resistance factor design (LRFD) approach for reliability based seismic design of rock slopes against wedge failures", *Proceedings of the 2013 Geo-Congress*, San Diego, CA, USA, March, pp. 582-591.
- Chen, Z.Y., Wang, X.G. and Yang, J. (2005), "Rock slope stability analysis-theory, methods and programs", *China Water Power Press*, Beijing, China.
- Choi, S.O. and Chung, K. (2004), "Stability analysis of jointed rock slopes with the Barton-Bandis constitutive model in UDEC", *Int. J. Rock Mech. Min. Sci.*, **41**(1), 581-586.
- Feng, P. and Lajtai, E.Z. (1997), "Probabilistic treatment of the sliding wedge with EzSlide", *Eng. Geol.*, **50**(1-2), 153-163.
- Fenton, G.A. and Griffiths, D.V. (2008), *Risk Assessment in Geotechnical Engineering*, John Wiley & Sons Inc.
- He, J.M., Xu, M.H., Ma, D.X. and Cao, J. (2012), "The application of Barton structural plane shear strength formula in Murum Hydropower Station, Malaysia", *Resour. Environ. Eng.*, **5**, 542-544.
- Hoek, E. (2007), "Practical rock engineering", Accessed on March 4, 2010
<http://www.rocksolid.com/hoek/PracticalEngineering.asp>
- Hoek, E. and Bray, J. (1981), *Rock Slope Engineering*, (3rd Ed.), The Institution of Mining and Metallurgy, London, UK, 358 p.
- Jaeger, J.C. (1971), "Friction of rocks and stability of rock slope", *Geotechnique*, **21**(2), 97-134.
- Kliche, C.A. (1999), *Rock Slope Stability*, Society for Mining Metallurgy, Littleton, CO, USA.
- Ladanyi, B. and Archambault, G.A. (1970), "Simulation of shear behaviour of a jointed rock mass", *Proceedings of the 11th US Symposium on Rock Mechanics*, Berkeley, CA, USA, June, pp. 105-125.
- Li, Y.H., Peng, Z.B., Zhong, Z.Q., He, Z.M. and Peng, W.X. (2009), "Strength prediction for rock mass based on Barton-Bandis nonlinear failure criterion", *J. Central South Univ. (Science and Technology)*, **40**, 1388-1391.
- Ling, H.I. and Cheng, A.H.D. (1997), "Rock sliding induced by seismic force", *Int. J. Rock Mech. Min. Sci.*, **34**(6), 1021-1029.
- Liu, M.W., Fu, H. and Wu, J.L. (2005), "Current situation of determination methods of shear strength parameters of rock-mass discontinuities and new thoughts", *J. Chongqing Jiaotong Univ.*, **24**, 65-67.
- Luo, Q., Li, L. and Zhao, L.H. (2010), "Quasi-static analysis on the seismic stability of anchored rock slope with the effect of surcharge and water pressure conditions", *Rock Soil Mech.*, **31**, 3585-3593.
- Ma, S.C., Li, H.Y. and Ouyang, Y.Q. (2008), "Types and cause analysis of traffic engineering damage

- during the ice disaster”, *J. Inst. Disaster Prevent. Sci. Technol.*, **10**, 5-8.
- Miller, S.M. (1988), “Modeling shear strength at low normal stresses for enhanced rock slope engineering”, *Proceedings of the 39th Annual Highway Geology Symposium*, Salt Lake City, UT, USA, August, pp. 346-356.
- Nagpal, A. and Basha, B.M. (2012), “Reliability analysis of anchored rock slopes against planar failure”, *Proceedings of Indian Geotechnical Conference*, New Delhi, India, December, pp. 1-4.
- Rocscience (2003), Roc-Plane – Planar sliding stability analysis for rock slopes; Verification Manual, *Geomechanics Software and Research, Rocscience Inc.*, Toronto, ON, Canada.
- Sharma, S. and Basha, B.M. (2012), “Reliability based seismic design of rock slopes against wedge failure: load resistance factor design (LRFD) approach”, *Proceedings of Soil Proceedings of Indian Geotechnical Conference*, New Delhi, India, pp. 5-8.
- Sharma, S., Raghuvanshi, T.K. and Anbalagan, R. (1995), “Plane failure analysis of rock slopes”, *Geotech. Geol. Eng.*, **13**(2), 105-111.
- Shu, J.S., Wang, X.Z. and Zhou, Y.Y. (2004), “Improving on assumption for water pressure distributing on failure surface in rock slope”, *J. China Univ. Min. Technol.*, **33**, 509-512.
- Shukla, S.K. and Hossain, M.M. (2011a), “Analytical expression for factor of safety of an anchored rock slope against plane failure”, *Int. J. Geotech. Eng.*, **5**(2), 181-187.
- Shukla, S.K. and Hossain, M.M. (2011b), “Stability analysis of multi-directional anchored rock slope subjected to surcharge and seismic loads”, *Soil Dyn. Earthq. Eng.*, **31**(5-6), 841-844.
- Shukla, S.K., Khandelwal, S., Verma, V.N. and Sivakugan, N. (2009), “Effect of surcharge on the stability of anchored rock slope with water filled tension crack under seismic loading condition”, *Geotech. Geol. Eng.*, **27**(4), 529-538.
- Tang, H.M. and Chen, H.K. (2008), “Revised method of water pressure in control fissure of perilous rockmass”, *The Chinese J. Geol. Haz. Control*, **19**, 86-90.
- Wei, F.Q., Zhao, L.N., Jiang, Y.H., Yang, X.D., Ding, M.T. and Chen, H. (2008), “The disaster of snow storm and frozen rain and its influence on mountain hazards”, *J. Mount. Sci.*, **3**, 253-254.
- Wu, H.B., He, Z.P. and Cao, W.W. (2011), “Stability study of slope with planar failure based on different water pressure distributions”, *Rock Soil Mech.*, **32**, 2493-2499.
- Wyllie, D.C. and Mah, C.W. (2004), *Rock Slope Engineering*, (4th Ed.), Spon Press, London, UK.
- Yin, Z.Q. (2008), “Influence on geological disasters of the extreme climate event of spring 2008 in China”, *J. Inst. Disast. Prevent. Sci. Technol.*, **10**, 20-24.
- Zhang, Y.X., Song, X.C. and Wang, G.L. (2010), “Overturning stability analysis of rock slope under extreme snow disasters conditions”, *Chinese J. Rock Mech. Eng.*, **6**, 1164-1171.
- Zhang, Y.X., Wang, Y.B. and Song, X.C. (2011), “Sliding stability analysis of bedding rock slope considering extreme snow disasters”, *J. Disaster Prevent. Mitigation Eng.*, **4**, 351-357.
- Zhao, J. (1998), “A new JRC-JMC shear strength criterion for rock joint”, *Chinese J. Rock Mech. Eng.*, **17**, 349-357.
- Zhao, L.H., Luo, Q., Li, L., Dan, H.C. and Luo, S.P. (2011), “Stability of subgrade slope along river subjected to water level fluctuations and stream erosion”, *J. Highway Transport. Res. Develop.*, **5**(2), 1-9.

Appendix: The details of the trigonometric calculations of slope geometry

From Fig. 2, the length of the upper slope surface L_{CD} can be expressed as follows

$$L_{CD} = \frac{B}{\cos \alpha}. \quad (\text{A1})$$

From Fig. 2, the length of tension crack L_{DE} and the length of failure plane L_{EF} can be expressed as follows

$$L_{DE} = \frac{L_{DG}}{\sin(\delta - \theta)} \sin(\theta - \alpha) \quad \text{and} \quad (\text{A2})$$

$$L_{EF} = L_{FG} - L_{EG}, \quad (\text{A3})$$

where

$$L_{DG} = L_{CG} - L_{CD}, \quad (\text{A4})$$

$$L_{CG} = \frac{L_{CF}}{\sin(\theta - \alpha)} \sin(\beta - \theta), \quad (\text{A5})$$

$$L_{FG} = \frac{L_{CF}}{\sin(\theta - \alpha)} \sin(\pi + \alpha - \beta), \quad (\text{A6})$$

$$L_{CF} = \frac{H}{\sin \beta} \quad \text{and} \quad (\text{A7})$$

$$L_{EG} = \frac{L_{DG}}{\sin(\delta - \theta)} \sin(\pi + \alpha - \delta) \quad (\text{A8})$$

where L_{DG} , L_{FG} , L_{EG} , L_{CG} , L_{CF} is the length of the slope geometry DG , FG , EG , CG , CF respectively.

The area of wedge A_{CFG} can be expressed as follows

$$A_{CFG} = \frac{L_{FG} \cdot L_{CF}}{2} \sin(\beta - \theta). \quad (\text{A9})$$

The area of wedge A_{EDG} can be expressed as follows

$$A_{EDG} = \frac{L_{DG} \cdot L_{EG}}{2} \sin(\theta - \alpha). \quad (\text{A10})$$

The area of wedge A_{CDEF} can be expressed as follows

$$A_{CDEF} = A_{CFG} - A_{EDG}. \quad (\text{A11})$$

As shown in Fig. 1, the weight of the sliding wedge W_{CDEF} is calculated from the following

$$W_{CDEF} = \gamma_R \cdot A_{CDEF}, \quad (\text{A12})$$

where γ_R is the unit weight of the rock (kN/m^3).